

# Supporting Information

## Fabrication of Visible Light-Induced Antibacterial and Self-Cleaning Cotton Fabrics Using Manganese Doped TiO<sub>2</sub> Nanoparticles

Muhammad Zahid<sup>\*,†</sup>, Evie L. Papadopoulou<sup>\*,†</sup>, Giulia Suarato<sup>†,‡</sup>, Vassilios D. Binas<sup>§,⊥</sup>, George Kiriakidis<sup>§,⊥</sup>, Iosifina Gounaki<sup>¶</sup>, Ourania Moira<sup>¶</sup>, Danae Venieri<sup>¶</sup>, Ilker S. Bayer<sup>†</sup> and Athanassia Athanassiou<sup>†</sup>

<sup>†</sup> Smart Materials and <sup>‡</sup>In Vivo Pharmacology Facility, Istituto Italiano di Tecnologia, Genova 16163, Italy

<sup>§</sup> Institute of Electronic Structure and Laser (IESL), Foundation of Research and Technology-Hellas (FORTH), Vasilika Vouton, GR-70013 Heraklion, Greece

<sup>⊥</sup> Department of Physics, University of Crete, GR-70013 Heraklion, Greece

<sup>¶</sup> School of Environmental Engineering, Technical University of Crete, Chania 73100, Greece

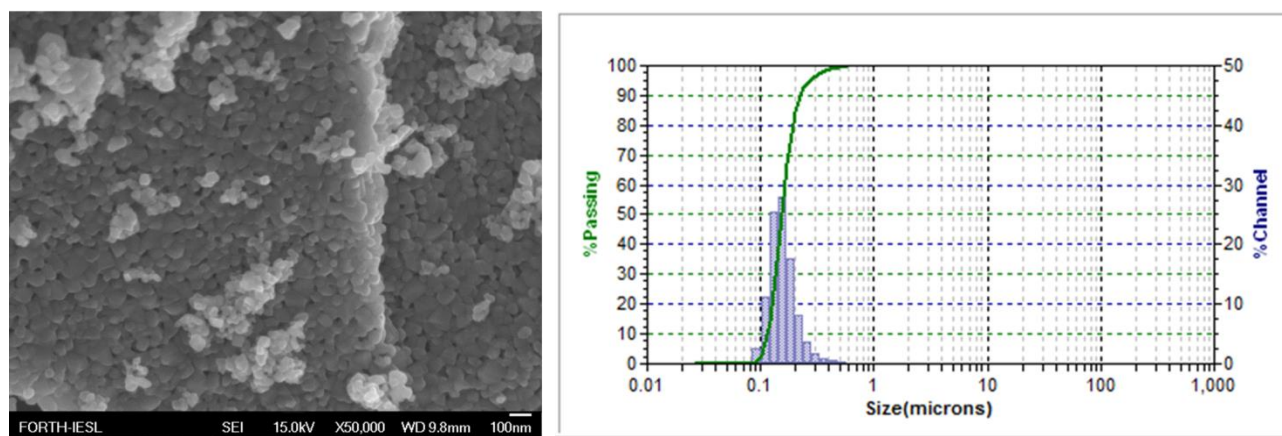
\*Corresponding authors;

Evie L. Papadopoulou; [paraskevi.papadopoulou@iit.it](mailto:paraskevi.papadopoulou@iit.it)

Muhammad Zahid; [Muhammad.zahid@iit.it](mailto:Muhammad.zahid@iit.it)

## **1. TiO<sub>2</sub>:Mn particle size distribution**

Figure S1 reports the High-Resolution SEM imaging (left panel) and the particle size distribution (right panel) of the TiO<sub>2</sub>:Mn nanoparticles. As seen on the right panel, the diameter of the nanoparticles ranges from ~90 nm to ~400 nm, with average diameter ~150 nm.



## **2. Hydrophobic properties**

Water repellency or hydrophobicity of the treated cotton fabrics was characterized by static water contact angle (WCA) using OCAH-200 DataPhysics contact angle instrument (Germany). Gastight 500  $\mu$ L Hamilton precision syringe with blunt needle of 0.52 mm internal diameter was used for droplet dispersion. The WCA of a 5  $\mu$ L droplet volume was measured after 30 s of droplet deposition. From each sample a strip of 1 $\times$ 5 cm<sup>2</sup> was cut and attached to contact angle table with double sided adhesive tape to get a wrinkle free surface for WCA measurements. Static WCAs at 10 different positions on each sample were measured and reported as mean values with standard deviations. For time dependent study of water spreading on untreated and TiO<sub>2</sub>:Mn nanoparticles (NPs)/PDMS coated fabrics were also conducted using a water blob of 200  $\mu$ L.

As shown in Figure S2a, PDMS coated fabrics demonstrate different WCAs depending on their TiO<sub>2</sub>:Mn NPs mass fractions. Sample NPs0 with only PDMS coating displays a WCA of 134 $^\circ$ , whereas, an increase in WCA is observed with higher NPs mass fraction in coating formulation. Such as, sample NPs25 with 25 wt.% mass fraction of NPs demonstrates a highest WCA of 145 $^\circ$ . On the other hand, the sample NPs50 with 50 wt.% mass fraction of NPs maintains a WCA of 140 $^\circ$  on its surface. Although, all the treated samples exhibit good hydrophobicity for short time (1 m), prolonged contacts with water blob of 200  $\mu$ L was able to spread out and impregnate the fabric's

surface as sample NPs50 is shown in Figure S2b. This wetting behavior of PDMS coatings have been investigated in previous studies as well.

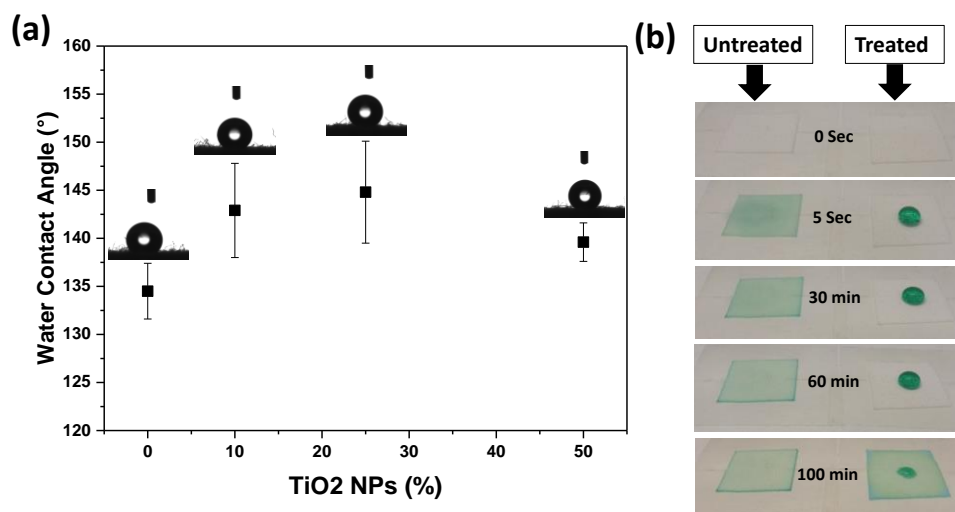


Figure S2. (a) WCA of treated cotton fabrics with increasing NPs mass fractions. (b) Time dependent spreading of colored water droplets on the surface of untreated and TiO<sub>2</sub>:Mn NPs/PDMS treated fabrics (sample NPs50).

### 3. Breathability

Breathability of the prepared cotton fabrics was measured by water vapor permeability (WVP), using metallic permeation cells. The WVP of fabrics was determined at 25 °C and under 100% relative humidity gradient ( $\Delta RH\%$ ) according to the ASTM E96 standard protocol. 450  $\mu\text{L}$  of distilled water (which generates 100% RH inside the permeation cell) was placed in each test permeation cell with a 7 mm inner diameter and a 10 mm inner depth. Fabrics were cut into circles and mounted on the top of the permeation cells. The permeation cells were placed in 0% RH desiccator with anhydrous silica gel (Sigma Aldrich) used as a desiccant agent. The water transferred through the fabric pores was determined from the weight change of the permeation cell every hour during the first 8 h using an electronic balance (0.0001 g accuracy). The weight loss of the permeation cells was plotted as a function of time. The slope of each line was calculated by linear fitting. Then, the water vapour transfer rate (WVTR) was determined as below<sup>1-3</sup>;

$$\text{WVTR (g m}^{-2} \text{ day}^{-1}) = \frac{\text{Slope}}{\text{area of the fabric}} \quad (1)$$

WVTR measurements were replicated three times for each fabric sample and the average WVP of the fabrics were calculated as follows;

$$\text{WVP (g m}^{-1} \text{ day}^{-1} \text{ Pa}^{-1}) = \frac{\text{WTVR} \times l \times 100}{\rho_s \times \Delta RH} \quad (2)$$

where  $l$  (m) is the fabric thickness, measured with a micrometer with 0.001 mm accuracy,  $\Delta RH$  (%) is the percentage relative humidity gradient, and  $p_s$  (Pa) is the saturation water vapour pressure at 25 °C (3168 Pa).

For WVTR and WVP measurements, untreated and Mn:TiO<sub>2</sub> NPs treated fabrics were compared. As shown in Figure S3, a comparison of WVTR (black) and WVP (red) is given for the respective samples. Highly hygroscopic cotton fabric demonstrates WVTR and WVP of 5160 g m<sup>-2</sup> day<sup>-1</sup> and 3.58 × 10<sup>-4</sup> g m<sup>-1</sup> day<sup>-1</sup> Pa<sup>-1</sup>, respectively. After functional coatings, a minor descending trend in moisture transfer rate and permeability are noticed in PDMS coated fabrics with increasing NPs mass fractions, as shown in Figure S3. For instance, WVTR and WVP of sample NPs50 are reduced to 4840 g m<sup>-2</sup> day<sup>-1</sup> and 3.36 g m<sup>-1</sup> day<sup>-1</sup> Pa<sup>-1</sup>, respectively. Nonetheless, the change in WVTR and WVP is not more than 6% for all NPs mass fractions as compared to untreated cotton fabric, as shown in Figure S3.

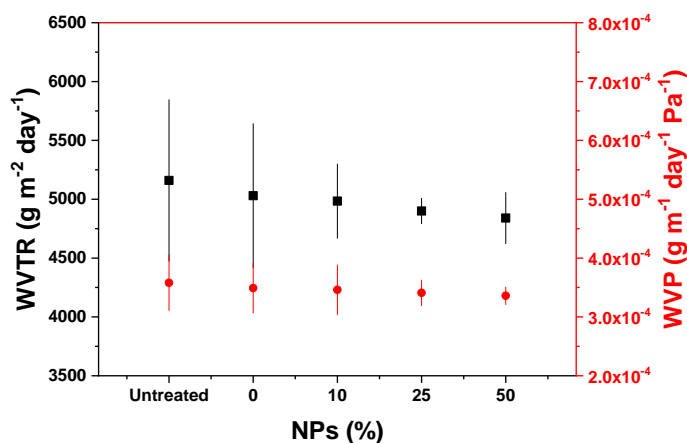


Figure S3. WVTR and WVP of untreated and different treated fabrics.

#### **4. Raman spectroscopy**

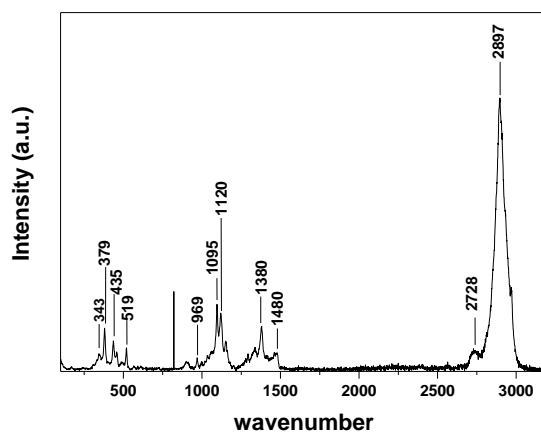


Figure S4. Raman spectra of untreated cotton fabric.

## 5. Stress-strain curves before and after washing

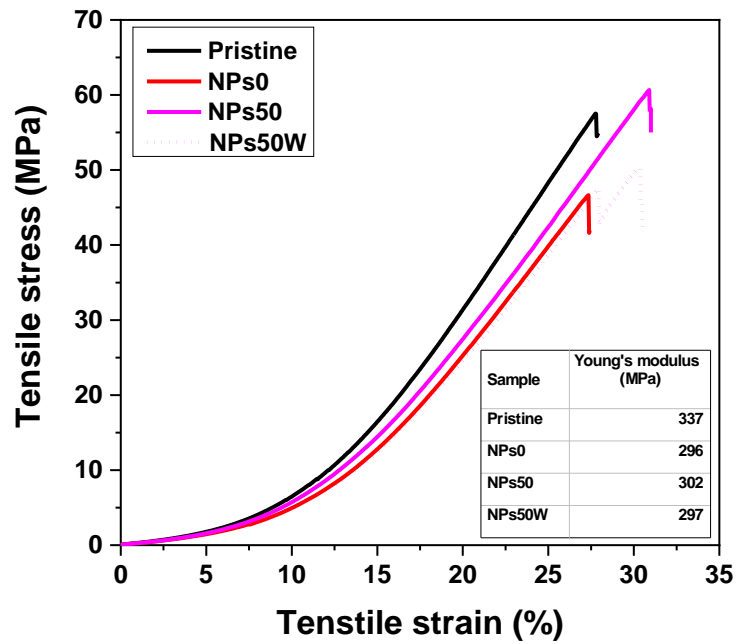


Figure S5. Mechanical properties of the sample NPs50 before and after 10 washing cycles (that is sample NPs50W). For comparison, untreated and pure PDMS treated (sample NPs0) cotton fabrics are also included.

## 6. Bacterial inactivation test

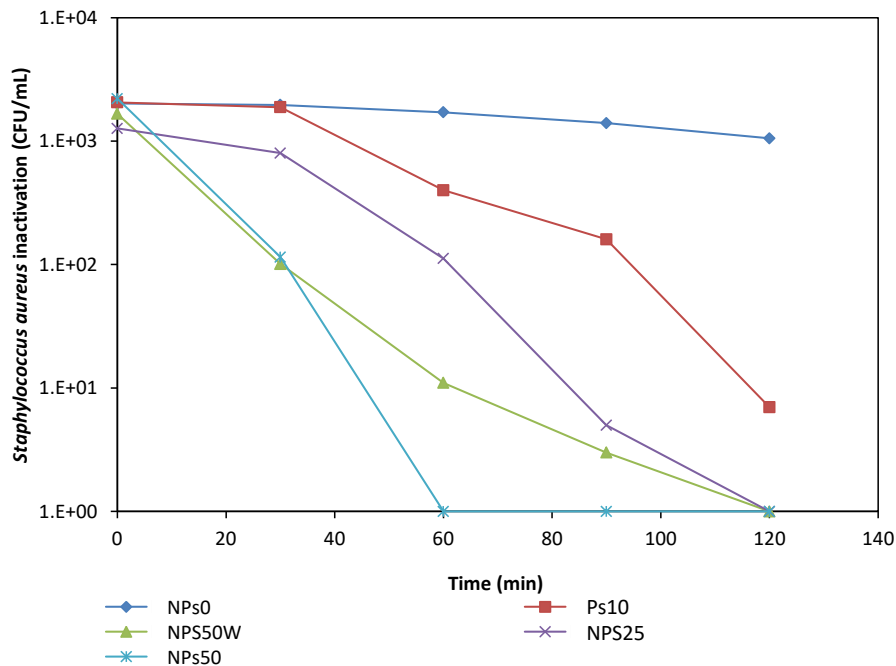


Figure S6. Inactivation of *Staphylococcus aureus* bacterium under sunlight.

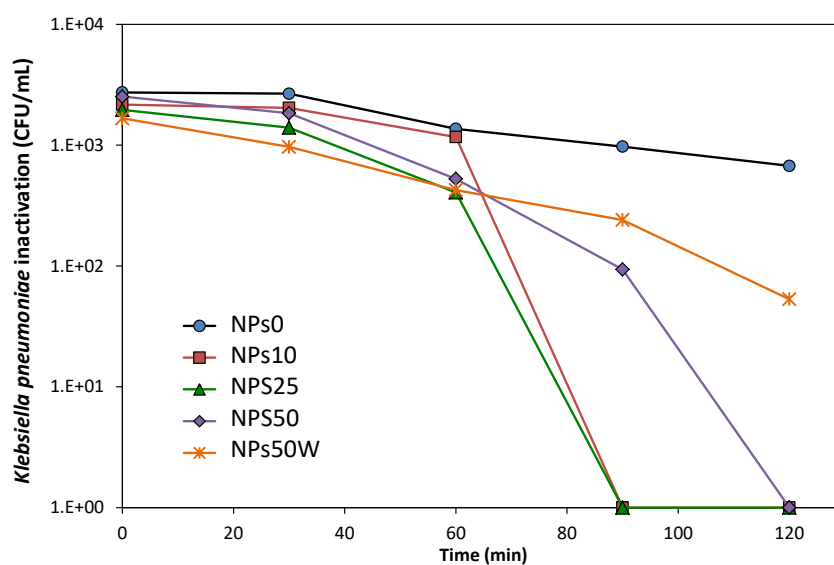


Figure S7. Inactivation of *Klebsiella pneumoniae* bacterium under sunlight.

### 7. Degradation of MB dye under UV irradiation (self-cleaning)

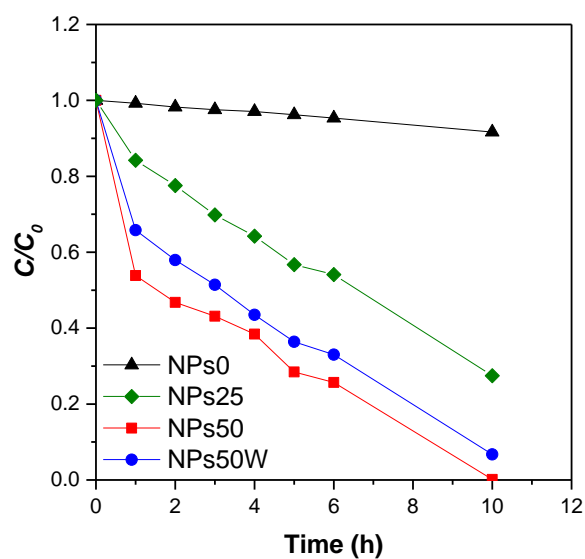


Figure S8. Degradation of MB dye stains by TiO<sub>2</sub>:Mn NPs coated cotton fabric under UV light irradiation. Reduction in relative concentration ( $C/C_0$ ) of MB model dye adsorbed on different samples is given as a function of UV irradiation time.

## 8. Degradation of MB dye in aqueous solution under UV irradiation (water purification)

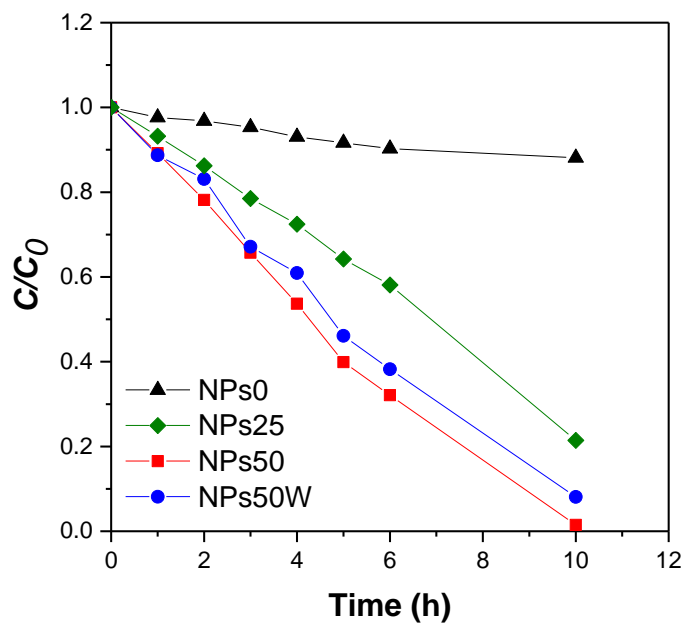


Figure S9. Degradation of MB in water (50 mL) by TiO<sub>2</sub>:Mn NPs coated cotton fabric under UV light irradiation. Reduction in relative concentration ( $C/C_0$ ) of MB model dye in aqueous solution by different coated samples is given as a function of UV irradiation time.

## References